

1 **Experimental Investigation on Thermal Performance of Underground** 2 **Refuge Chamber under Natural Convection and Ventilation**

3 Zujing Zhang^{a,b*}, Ting Jin^a, Liang Ge^b, Xing Liang^c, Hongwei Wu^d, Ruiyong Mao^{a**}

4 ^a College of Civil Engineering, Guizhou Provincial Key Laboratory of Rock and Soil Mechanics and
5 Engineering Safety, Guizhou University, Guiyang, 550025, China

6 ^b State Key Laboratory of Gas Disaster Detecting, Preventing and Emergency Controlling, Chongqing,
7 400037, China

8 ^c School of Computer Science and Mathematics, Kingston University London, KT1 2EE, United
9 Kingdom

10 ^d School of Physic, Engineering and Computer science, University of Hertfordshire, Hatfield, AL10
11 9AB, United Kingdom

12 *Corresponding author: email: zjzhang3@gzu.edu.cn. **Corresponding author: email: rymao@gzu.edu.cn.

13 **Abstract:** Thermal performance of densely populated underground buildings is normally influenced
14 by various factors, including the surrounding rock (SR), ventilation, and indoor heat sources. It is
15 recognized that little experimental studies on thermal control for the above building was reported. In
16 this article, a full-size 50-person mine refuge chamber (MRC) was newly constructed to test the
17 thermal performance under natural convection and ventilation. The heat ducts were used to simulate
18 the heat released from human body. Experimental results indicated that: (1) the intensity of the heat
19 transfer between rock and air increases with the rise in heat source rate and ventilation temperature
20 (VT), while it decreases as the initial surrounding rock temperature (ISRT) increases; (2) when
21 considering the joint temperature control of pre-cooled SR, it is recommended to reduce the VT linearly
22 during the evacuation period in order to ensure the thermal safety of personnel. During the non-refuge
23 period, the cold amount should be stored as far as possible into the shallow SR body to make full use
24 of it; (3) to ensure the thermal safety of an MRC with a capacity of 30 people, cooling measures lasting
25 96 hours are required when the ISRT exceeds 21.3 °C. In addition, when the ISRT reaches 27.6 °C, the
26 per capita ventilation is 0.19 m³/min, and the temperature is 26 °C, which can also meet the
27 requirements. This study provides experimental verification as a basis for future research on
28 underground space temperature control considering the influence of SR, thereby contributing to further
29 understanding in this field.

30 Key words: Mine refuge chamber; Initial surrounding rock temperature; Natural convection;
31 Ventilation; Thermal control.

Abbreviations

AIL	air inlet layout	IW	inner wall
EW	exterior wall	MRC	mine refuge chamber
HSI	heat source intensity	SR	surrounding rock
ISRT	initial surrounding rock temperature	SRT	surrounding rock temperature
IT	indoor temperature	VT	ventilation temperature

1. Introduction

Underground space plays a crucial role in saving land, relieving traffic pressure and improving resource utilization rate [1], broadening the scope of human activities [2], which is becoming a key issue for future urban development [3]. In recent years, the underground space has been actively developed [4-5], such as underground railway station [6-7], underground shopping mall [8-10], underground air-raid shelter [11-13], MRC [14-16] and other protective engineering [17]. As enclosed environments with functions of living and working, the underground building maintains a suitable indoor environment by natural or artificial with reasonable energy and cost-effective [18]. Unlike long-running underground confined spaces such as underground shopping mall, the underground air-raid shelter and MRC only operate during wartime or in the event of a mine accident, providing a safe environment for high-density people.

When the confined underground spaces are in operation, the gases and heat generated by people will make both the indoor temperature (IT) and relative humidity increase, exacerbating air deterioration in the MRC [19-20]. The indoor thermal environment directly affects the human thermal comfort and efficiency [21]. In China, in order to control the IT below 35 °C within 96 h, the underground refuge room is required to provide no less than 0.3 m³/min of air flow per capita [22-23]. As the primary heat source in MRCs, people primarily exist in two states, sitting and lying down, with relatively stable heat production values that can be determined to be 117 W [19, 24], 113~114 W [25], 125.87 W [26] and 117~128 W [27]. It is now generally accepted that the per capita heat production in a sitting position is 120 W [28]. In addition to the heat dissipation generated by people, the heat dissipation of the surrounding rock (SR) also has a significant effect on the rise in IT [19][29]. Gao et al. [30] built a basement model integrated with a long vertical earth-air heat exchanger system. Their research showed that for a MRC located in sandstone and buried at a depth of 400 m as well as supplied with air using surface boreholes, when the ISRT was 28.5 °C, the IT was controlled at approximately

1 30 °C after 96 h at a per capita airflow of 0.3 m³/min. Zhang et al. [28] established a validated numerical
2 model of a MRC and found that for a MRC built in a sandstone seam with ISRT of less than 27 °C, the
3 average air temperature will not exceed 35 °C in 96 h when the ventilation volume rate is 0.3 m³/min
4 per capita. Several methods can enhance the heat transfer include, but are not limited to, an increase in
5 the heat transfer area and the promotion of turbulence [31-33]. Zhang et al. [28] also found that the
6 temperature rise rate of a MRC was proportional to the heating rate, but inversely proportional to the
7 thermal conductivity, density and specific heat capacity of the rock, as well as the ventilation volume
8 rate and wall area.

9 The shallow coal resources are becoming depleted and gradually entering the deep mining stage
10 [34]. At the same time, the amount of the heat dissipation from the SR gradually increases [35].
11 Therefore, the influence of the SR cannot be ignored when controlling the temperature of the MRC.
12 Moreover, energy storage in the SR can also be utilized due to its safety and economic characteristics
13 [36]. In this way, energy storage in the SR can reduce winter heating and summer cooling energy
14 consumption while assisting in the thermal management of the underground mines [37]. Zhu et al. [38]
15 adopted a numerical method to simulate the natural cooling and heat regulation of the air flow, and
16 proposed to use the seasonal temperature difference of the SR to cool ventilation to reduce thermal
17 hazards. Yuan et al. [39] proposed a composite temperature control method of the SR cooling storage-
18 phase change heat storage in order to simultaneously meet the requirements of safe, passive and
19 reliable indoor cooling at high temperature MRC by establishing a numerical simulation model. Gao
20 et al. [40] continued their research and established a simplified numerical MRC model for intermittent
21 heat storage. Compared with continuous cooling storage, intermittent cooling storage has significant
22 energy-saving effect, which could improve the heat transfer performance and reduce the energy
23 consumption.

24 Existing studies have revealed that the temperature control characteristics of the underground
25 confined space under natural and forced convection conditions, as well as revealed the influence
26 mechanism of the enclosure structure on IT control. Even the SR is used as a new green carrier for
27 cold storage to control the IT, most of these studies conducted by numerical simulation lack of
28 experimental verification of the temperature control and SR storage characteristics under ventilation
29 conditions. Zhang et al. [29] explored the influence of the enclosure on the IT control by conducting a
30 1-hour heating experiment at 6000 W under natural convection conditions. Based on this experiment,

1 a numerical model was established to analyze the effects of ventilation, heating rate, and wall area on
2 the IT control [28]. However, there was some issues on the experimental work, such as the laboratory
3 was a shallow chamber buried 3 m underground with 1 m exposed surface and 0.4 m thick top wall,
4 and the experimental results were affected by the surface environment. Their experimental study did
5 not conduct on the forced convection. Regarding the experimental study on the simulation of the
6 temperature of the SR, Zhang et al. [41] investigated the temperature variation rules of the constant
7 temperature SR with an inner diameter of 0.8 m and an outer diameter of 1 m of the ventilation roadway
8 under different ventilation speeds through the self-designed transient heat transfer simulation
9 experimental device for the SR of the high geothermal roadway. In the real conditions, the heat
10 exchange often occurs between the roadway and SR, therefore, the temperature distribution of the SR
11 is usually uneven. However, the equipment did not pay attention to the temperature change of the non-
12 isothermal SR. Regarding the study of the coupled heat transfer characteristics of air and SR in
13 underground construction. The numerical models proposed by Li and Ding [35][42] were verified
14 against the actual measurements, but their research focuses on the thermal environment of open tunnels.
15 The experiment of this study can make up for the defects of the above research experiments.

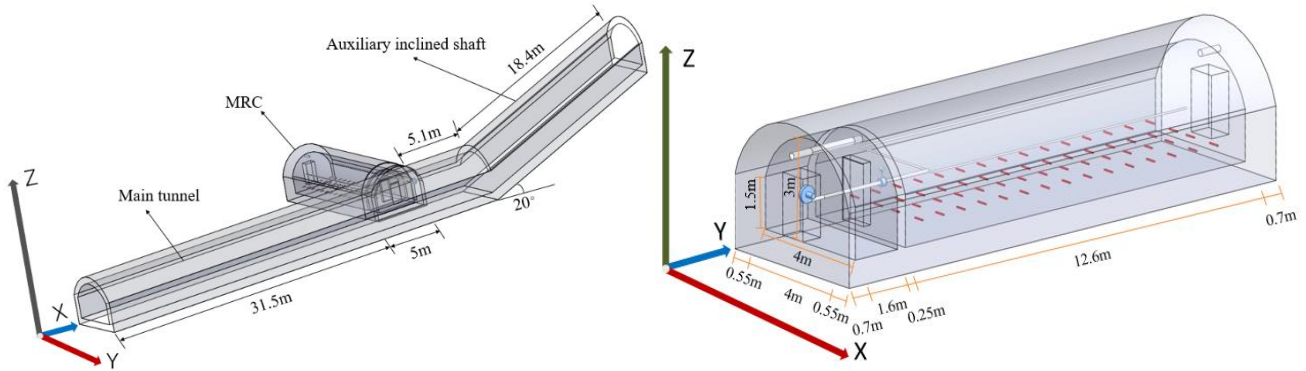
16 Compared with the numerical calculation method, the data of the simulation experiment is closer
17 to the real one. Therefore, in order to better explore the factors affecting the temperature of
18 underground confined space, this study is based on the experiment in underground simulated mine
19 with buried depth of more than 2 m. By using the heating tube to simulate the human heat dissipation,
20 it explores the temperature control performance of MRC and the cold storage characteristics of SR
21 under the condition of natural convection and mechanical ventilation. This study provides a basis for
22 further experimental verification through abundant experiments.

23 **2. Methodology**

24 **2.1 Experimental environment**

25 The MRC laboratory is situated within a simulated mine environment, specifically designed as a
26 prototype of a main tunnel-auxiliary inclined shaft configuration, as depicted in Figure 1 (a). The main
27 tunnel boasts dimension is 5 m in width and 40.6 m in length, featuring an arch-shaped cross-sectional
28 design. Connected to the main tunnel is an auxiliary inclined shaft with an inclination angle of 20° and
29 a length of 18.4 m. Positioned at distances of 31.5 m from the entrance of the main tunnel and 23.5 m

1 from the entrance of the inclined shaft, the MRC structure itself primarily comprises concrete material
 2 characterized by C30 strength properties, possessing a thermal conductivity value of $0.90 \text{ W}/(\text{m}\cdot^\circ\text{C})$,
 3 density measuring at $2636 \text{ kg}/\text{m}^3$, and specific heat capacity amounting to $970 \text{ J}/(\text{kg K})$. The floor
 4 exhibits a thickness measurement of approximately 0.6 m while both walls maintain minimum
 5 thicknesses reaching up to at least 0.55 m . Meanwhile, the roof showcases an increased thickness
 6 ranging between approximately $2\sim 3 \text{ m}$ due to its coverage with backfill soil.



7
 8 (a) The geometrical structure of part of mine

(b) MRC geometry structure



9
 10 (c) Main tunnel



(d) Auxiliary inclined shaft

11 Fig. 1 Scene diagram of the mine in the current study.

12 In general, the MRC laboratory is 15.85 m in length and 5.1 m in width. The refuge has a cross-
 13 section of 3 m (in height) by 4 m (in width), with vertical walls of 1.5 m in height and a perimeter of
 14 12.35 m of an arch. The MRC is divided by 3 walls into 2 spaces, a 12.6 m long living room and a 1.6
 15 m long transition room. The two walls connected to the external environment are 0.7 m in thickness,
 16 while the middle partition wall is 0.25 m in thickness. The size of the door frame in the middle of the
 17 three walls is 1.8 m in height and 0.9 m in width, and the bottom of the door frame is 0.3 m from the
 18 ground, as shown in Fig. 1 (b). The door is made of 2 mm stainless steel plate and filled with

1 polyurethane insulation material with a thickness of 0.04 m. The gaps are filled with polyurethane
2 foaming sealant.



3
4 (a) External roadway of MRC

(b) Interior of MRC

5 Fig. 2 Scene diagram of the MRC.

6 2.2 Experimental principle

7 The living room of the MRC laboratory covers an area of about 50 m², which can accommodate
8 50 people at maximum, this is based on the requirements that the per capita floor area is not less than
9 1 m² and 1.2 times of the coefficient is reserved. In practical underground works, a refuge of this size
10 is typically occupied by 30 to 50 people. In order to simulate the effect of the human heat dissipation
11 on the temperature control of the MRC for no less than 50 people, 60 copper heating tubes with fins
12 of 100 W, as shown in Fig. 3 (a), were used to simulate the human heat dissipation when the per capita
13 heat production rate was calculated at 120 W. The tubes, 0.35 m in length and 0.02 m in diameter, are
14 distributed in 4 rows of 15 columns in the living room. Among them, the two outermost columns of
15 the heating tubes are 0.7 m away from the wall at both ends, and the rest of the heating tubes are 0.8
16 m apart. The heating tubes near both sides of the wall are 0.4 m away from the wall, and the two rows
17 in the middle are 0.4 m apart. The working state of the heating tubes can be controlled through a power
18 control box, four different heat rates were considered, i.e., 3600 W, 4400 W, 5200 W and 6000 W,
19 respectively, to simulate the heat rate from 30, 37, 43 and 50 people, and the corresponding working
20 heating tubes are in columns 4 ~ 12, 3 ~ 13, 2 ~ 14 and 1 ~ 15.

21 To investigate the effect of the ventilation factors on the temperature control performance, a
22 pressurized air system of the MRC was constructed based on the actual engineering. The CZ-1500 W
23 series fan was adopted, see in Fig. 3(b), considering the requirement that the minimum ventilation rate

1 per capita acceptable for the mine air pressure system is $0.1 \text{ m}^3/\text{min}$ and the requirement that the per
2 capita air volume in the refuge room is not less than $0.3 \text{ m}^3/\text{min}$ [43]. The fan with rated flow rate of
3 $1530 \text{ m}^3/\text{h}$, power of 1.5 kW, voltage of 380 V, total pressure of 2400 Pa and speed of 2800 r/min
4 delivers outdoor fresh air into the MRC. The fresh air enters the transition room through a 2.5 m long
5 DN100 stainless steel ventilation duct, passes through a vortex flow meter, and then enters the living
6 room through a 1.8 m long DN100 stainless steel duct, finally discharges through a tee transfer to the
7 air supply ducts on both sides. The air supply duct of DN50 with 9.6 m in length on both sides is 1.8
8 m in height from the ground and 0.2 m from the wall. For the purpose of analyzing the effect of air
9 inlets on the ventilation and temperature control performance of the MRC, five DN25 air inlets with
10 distance of 2 m and twenty DN12.5 air inlets with distance of 0.5 m were reserved on each-side air
11 supply duct. Three different air inlet layouts (AILs) were considered in the current study, as shown in
12 Fig. 4. When DN12.5 is used, the fresh air is directly sent into the MRC. When DN25 is used, two
13 ways of direct air supply and diffused air supply through silencer are considered. The polluted air is
14 discharged to the outside through the outlet duct of DN200 located 2.65 m above the ground on the
15 walls at both ends.

16
17
18



(a) Heating tube



(b) Fan



(c) Silencer

Fig. 3 Photo of experimental equipment.

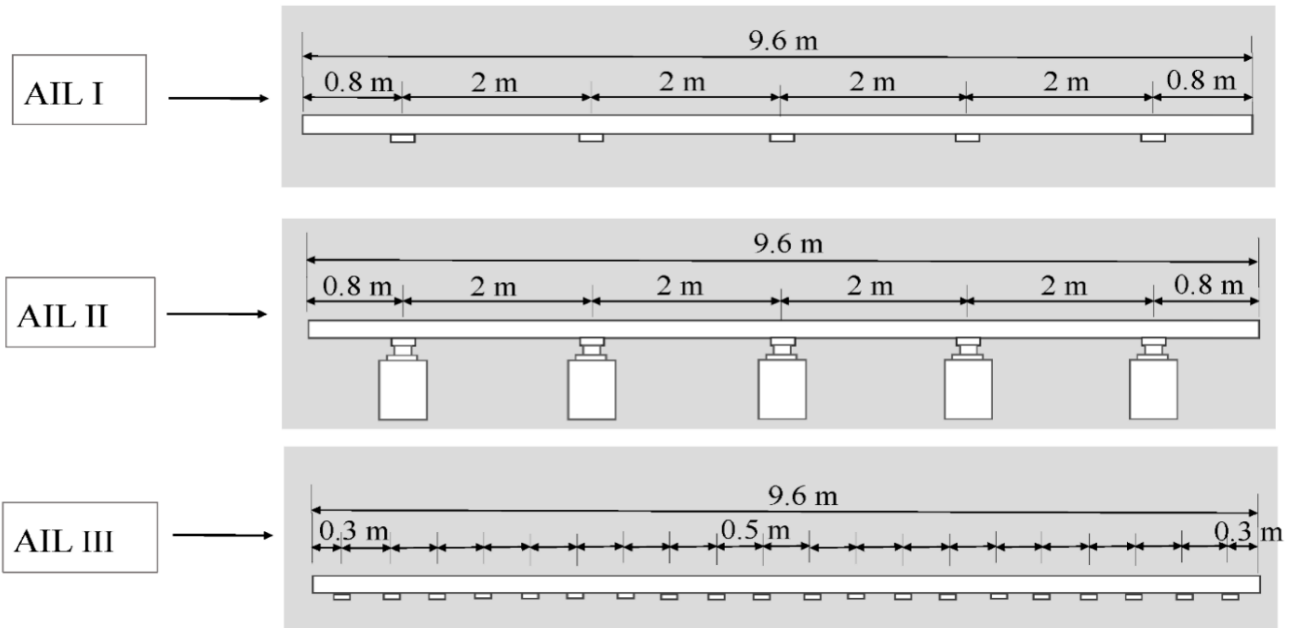


Fig. 4 Schematic diagram of AILs.

In the current study, the following assumptions and limitations are made: (1) it was assumed that the heat absorption or release of the thinnest wall selected represents the heat absorption or release of the envelope. Since the concrete thickness of the square wall of the mine is not the same, and the wall area before and after the MRC is small, thus, in order to get the wall affected by the IT, the thinnest wall (55 cm in thickness) on the left side of the MRC was selected for testing; (2) assuming that the heat dissipation of the heating tube is equivalent to that of the human body, we only considered the impact of the human heat dissipation on the temperature control while disregarding the influence of the actual human surface area; (3) we assumed that the average value derived from the instantaneous air volume data every 5 minutes over a 24-hour period represents the total air supply volume within this duration. However, due to employing a constant volume fan whose airflow is dependent on factors such as air temperature, pressure, and motor speed, it became challenging to maintain a fixed air supply volume. So the data was processed in this way.

2.3 Cases design

The two-month experiment was conducted from August 31 to October 31, 2022. The measurement duration of each case was 24 h. The setting of each case is shown in Table 1. Cases 1 to 4 tested the temperature control performance of the MRC under natural convection with different heat source intensity (HSI), with the fan off during these cases. Cases 5 to 12 tested the temperature control performance of the MRC for different HSI and different AILs. Case 13 tested the ventilation and cold

1 storage performance of the SR in the MRC without heat source. The IRST is the average temperature
 2 of the SR measurement point. The air supply temperature varies with the ambient temperature in the
 3 roadway. Therefore, the wind temperature range was 18~32 °C. For the 50 people room in this study,
 4 the air volume of about 350 m³/h meets the standard of not less than 0.1 m³/min per capita.

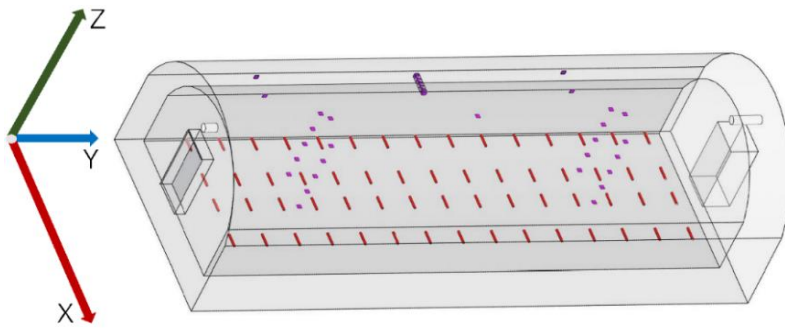
5 Table 1. The settings of each case:

NO.	AIL	HSI / W	ISRT / °C
1	/	3600	21.3
2	/	4400	21.7
3	/	5200	21.8
4	/	6000	23.1
5	AIL II	3600	23.3
6	AIL III	3600	23.2
7	AIL I	3600	27.2
8	AIL III	3600	27.6
9	AIL I	3600	25.8
10	AIL I	4400	22.5
11	AIL I	5200	23.9
12	AIL I	6000	23.3

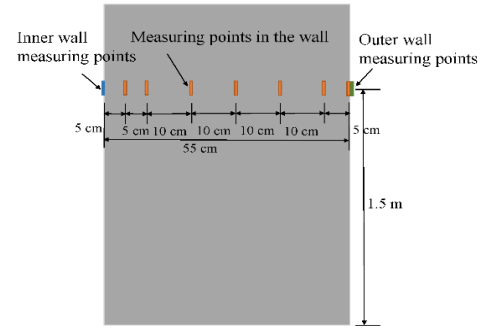
6

7 **2.4 Data acquisition**

8 To obtain the variation characteristics of the IT in the MRC, 20 measuring points were set at the
 9 five levels 0.5, 1, 1.5, 2 and 2.5 m above the floor, respectively, and three measuring points were set at
 10 3.0 m above the ground, as shown in Fig. 5 (a). In order to obtain the variation characteristics of the
 11 surrounding rock temperature (SRT) in the MRC, six temperature measuring points were arranged on
 12 both the inside and outside surfaces of one wall, three heat flux measuring points were arranged on the
 13 inner wall (IW) surface, and seven temperature measuring point was arranged at 5, 10, 20, 30, 40, 50
 14 and 55 cm inside the wall, as shown in Fig. 5 (b).



(a) Three-dimensional map of measuring points





(b) Measuring points of wall

Fig. 5 Maps of measuring points in the MRC.

Instantaneous air volume and VT were measured by integrated display vortex flowmeter. The data collection of the instantaneous air volume and VT can be transmitted transparently through module. The temperature IW and exterior wall (EW), the temperature at the height of 3.0 m inside the room and the heat flow of the IW were measured by the thermal performance testing equipment of the building envelope of the Chinese Academy of Architectural Sciences. The temperature at five heights of 0.5, 1, 1.5, 2 and 2.5 m and the temperature inside the SR were measured by JK4032 temperature acquisition instrument of Jinke. The performance parameters of each measuring instrument are shown in Table 2. It should be noted that the “R” in Table 2 stands for real-time readings.

Table 2. The performance parameters of each measuring instrument.

Instrument name	Merchant	Measurement parameters	Measurement range	Thermocouple type	Measurement accuracy	Picture
Vortex flowmeter	Shun lai da	Air temperature Air volume	-40~260 °C 133~1700 m ³ /h		±1.5%R ±1%R	
Temperature acquisition device for SRT	China Academy of Architectural Sciences	Temperature Heat flow	100~100 °C 0.3~200.00 mV	PT1000	±0.1 °C ±0.1 mV	

Temperature acquisition device for IT

Jinke

Temperature

200~850 °C

PT100

± (0.5% R + 1) °C



1

2 The heat transfer coefficient of the envelope structure in each working condition was measured
3 by the heat flux meter and calculated by the following formula [44]:

4
$$K=1/(R+R_e+R_i) , R=(T_i+T_e)/q \dots\dots\dots (1)$$

5 where R is the absolute value (positive value); K is the heat transfer coefficient; R is the thermal
6 resistance, m²·k /W; T_i is the mean temperature inside the wall, °C; T_e is the mean temperature outside
7 the wall, °C; R_i is the heat transfer resistance inside the wall, m²·°C/W, normally 0.11; R_e is the heat
8 transfer resistance outside the wall, m²·°C/W, normally 0.04; q is the average heat flow, W.

9 In order to minimize the measurement error, when processing the experimental data, the average
10 value of the four measuring points at five heights were taken as the temperature of these five heights.
11 The average temperature of the three measuring points with the height of 0 m and 3 m was taken as
12 the temperature of these two heights. The average temperature of the three measuring points on the IW
13 and the EW was taken as the temperature inside and outside the wall. The average value of the three
14 heat flow gauges on the IW was taken as the wall heat flow value. The temperature recording interval
15 of each measuring point is five minutes. The average value of 24 h instantaneous air volume was taken
16 as the air supply volume.

17 **2.5 Governing equations**

18 Under the condition of air pressure in the cooling mine, the average IT of the refuge after
19 ventilation for 1 h can be calculated as follows [23]:

20
$$Ta(\tau)=[(1.353Tv+1.301T_{isrt}+4.628Q) \times 102+0.7e0.002G$$

21
$$0.155]\sqrt{\tau}+0.271Tv+0.711T_{isrt}+3.339 \times 103G +0.786Q+4.069$$

22 where, Ta is the IT in the MRC, °C; τ is the ventilating time, h; T_v is the VT, °C; T_{isrt} is the
23 ISRT, °C; G is the ventilation rate, m³/h; Q is the HSI generated by people, kW.

24 **2.6 Experimental uncertainty**

25 This experiment mainly focused on the IT of the MRC with internal heat source under the

1 ventilation condition, thus, the measurement data of Case 5 was selected to calculate the experimental
 2 uncertainty. The experimental uncertainty of the test data is calculated by Eq. (4) [45]. If the
 3 relationship between dependent variables R and the independent variables x_1, x_2, \dots, x_n can be
 4 expressed as:

$$R = f(x_1, x_2 \dots x_n) \quad (3)$$

6 Then the uncertainty of the dependent variable R can be defined as follows:

$$\sigma_R = \sqrt{\sum_1^n \left(\frac{\partial R}{\partial x_i} \sigma_{x_i} \right)^2} \quad (4)$$

8 where, $\sigma_{x_1}, \sigma_{x_2}, \dots, \sigma_{x_n}$ is the direct uncertainty of x_1, x_2, \dots, x_n , respectively.

9 Table 3. The uncertainty of the measurement parameters and calculation parameters:

Item	Units	Range	Uncertainty
Measured parameters			
VT	°C	19.5~22.5	±1.5%
IRST	°C	19.2~28.3	±0.1 °C
Ventilation rate	m ³ /h	340~360	±1%
Temperature of EW	°C	18.3~19.9	±0.1 °C
Temperature of IW	°C	28.6~30.2	±0.1 °C
Heat flux	mV	4.2~9.6	±0.1 mV
Calculated parameters			
IT	°C	30~35.6	0.6 °C
Heat transfer coefficient			0.119

11 2.7 Experimental procedure

12 The research objective of the present study was to reduce the IT within 96 h to below 35 °C, and
 13 the IT at 1.5 m height was close to the average temperature of different indoor heights. Therefore, for
 14 the ventilation cooling experiment under the condition of forced convection and internal heat source,
 15 the experiment started when the IT was 35 °C at a height of 1.5 m. The main operation steps in the
 16 experiment were as follows:

17 (1) Cases 1~4: heating experiment under the condition of natural convection and internal heat
 18 source.

1 (a) Prior to the experiment, ensure the normal operation of all equipment and the normal data
2 recording, turn on the fan to reduce the wall temperature to similar to the air supply temperature, close
3 the outlet to prevent the indoor air circulation, and close the laboratory door;

4 (b) The heating tube begins to heat up;

5 (c) After 24 h of experiment, turn off the heating tube, and save the data.

6

7 (2) Cases 5 ~ 12: ventilated cooling experiment with internal heat source.

8 (a) Prior to the experiment, ensure the normal operation of all equipment and the normal data
9 recording, turn on the fan, reduce the wall temperature to similar to the air supply temperature, and
10 close the laboratory door;

11 (b) Open the heating tube and heat the IT to the level of 1.5 m, and the average temperature of
12 each measuring point is not less than 35 °C;

13 (c) Adjust the HSI to the set value of the corresponding case, and start the fan for cooling;

14 (d) After 24 h of experiment, shut down the fan, turn off the heating tube, and save the data.

15

16 (3) Case 13: ventilated cooling experiment without internal heat source.

17 (a) Prior to the experiment, ensure the normal operation of all equipment and the normal data
18 recording. After closing the laboratory door, open the heating tube to heat the IT to the level of 1.5 m,
19 and the average temperature of each measuring point is not less than 35 °C;

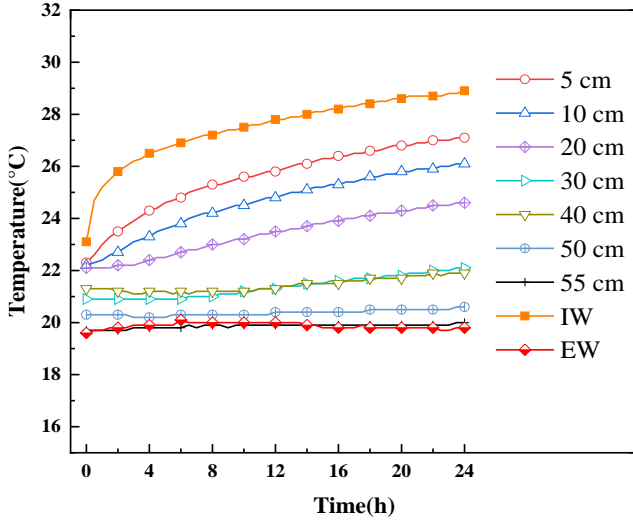
20 (b) Turn off the heating tube and turn on the fan for cooling;

21 (c) After 24 h of experiment, shut down the fan, turn off the heating tube, and save the data.

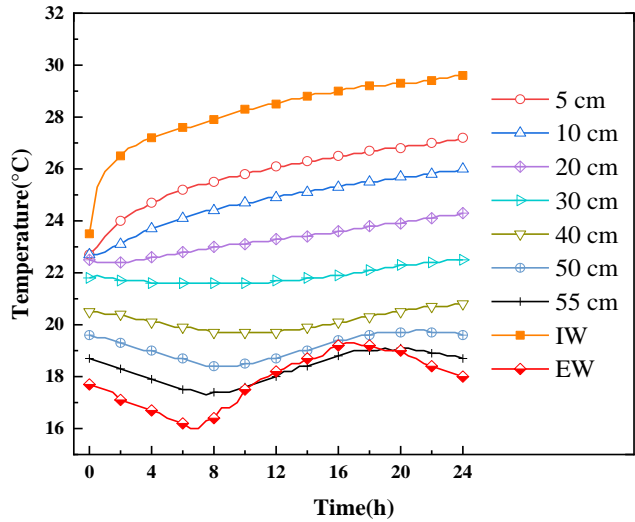
1 3. Results

2 3.1 Temperature control characteristics of MRC under natural convection

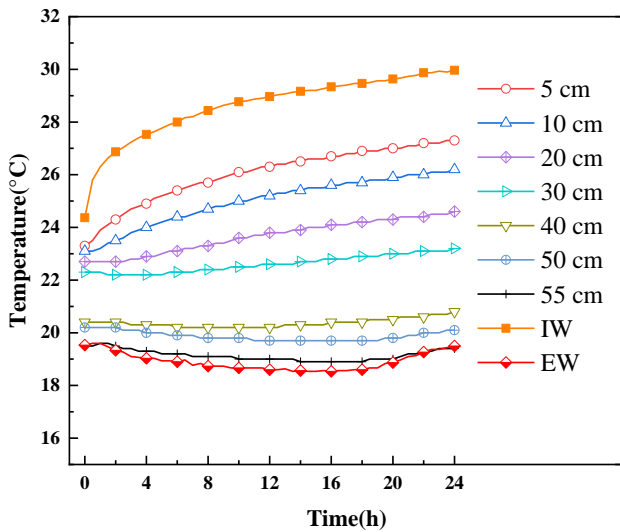
3 3.1.1 Characteristics of SRT variation under natural convection



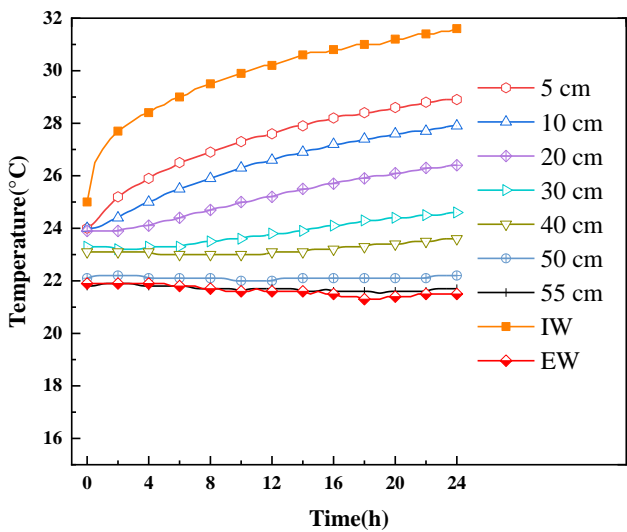
4 (a) Case1: HSI 3600 W, ISRT 21.3 °C



5 (b) Case2: HSI 4400 W, ISRT 21.7 °C



6 (c) Case3: HSI 5200 W, ISRT 21.8 °C



7 (d) Case4: HSI 6000 W, ISRT 23.1 °C

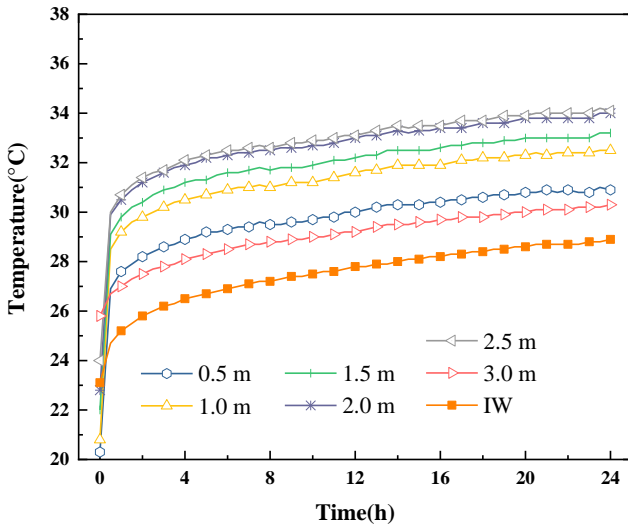
8 FIG. 6 SRT changes with different HSI under natural convection

9 Fig. 6 (a) ~ (d) plot the temperature curves of the SR within 24 h for different HSI of 3600 W,
10 4400 W, 5200 W and 6000 W under natural convection, respectively. As can be seen from Fig. 6 (a) ~
11 (d), at initial stage of the test, the rock temperature gradually decreases from inside to the outside,
12 which indicates that the temperature inside the SR is non-uniform. The temperature difference between
13 the inner and exterior surface walls was about 3 ~ 4 °C, which was caused by the short-term heating
14 and natural recovery experienced in the MRC prior to the test. In addition, the surface temperature of

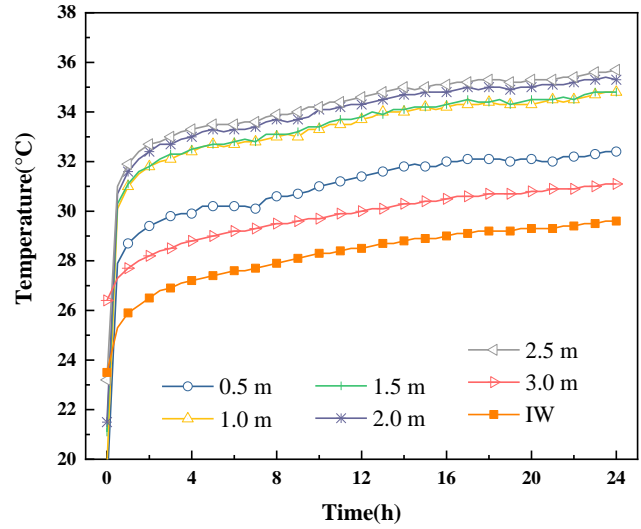
1 the EW of Case 1 and Case 4 was almost stable during the test, while there was a slight change in Case
2 3 and a more obvious change in Case 2. This phenomenon was caused by the change of the roadway
3 temperature during the test. As can be seen from Fig. 6 (a) ~ (d), the temperature of IW increases
4 approximately linearly within 0.5 h at the initial heating stage and then slowly rises, which is caused
5 by the dynamic heat transfer process of indoor air and SR surface from unstable state to relatively
6 stable state. Along with the heating time, the SRT gradually increased from inside to the outside, which
7 indicated that the low-temperature SR has a better ability to absorb the indoor heat. However, due to
8 the thermally inert of SR, the tendency of temperature increases in the MRC gradually slowed down.
9 As can be seen from Fig. 6 (a) and (d), the SRT at 0.55 m changes slightly after 22 h of the test, which
10 indicated that the heat-regulating circle of the SR was within 0.55 m when the MRC was heated for 22
11 h. It should be noted that the radius of the heat regulating ring usually refers to the distance between
12 the center of the MRC and the temperature in the rock, but the radius of the heat regulating ring referred
13 to here is the distance from the IW to the rock whose temperature has changed.

14 In order to compare the effect of HSI on the dynamic heat transfer strength of the SR and air, the
15 change of the surface temperature of the SR from 2 to 22 h after the heat transfer process between the
16 SR and air reached dynamic equilibrium was used as a reference. The surface SRT increased by 2.9, 4,
17 3.1 and 3.7 °C for HSI of 3600, 4400, 5200 and 6000 W, respectively. In addition, the heat transfer
18 coefficients of Case 1-4 measured by the thermal performance testing equipment were 2.771, 2.800,
19 3.525, and 3.924 W/(m²·°C), respectively. Among them, when the HSI was 4400 W, the temperature
20 gradient of the IW was larger because the VT was affected by the external environment temperature.
21 The temperature of the EW was also affected by the temperature of the external environment, therefore
22 the measured heat transfer coefficient was also small. However, the other three operating conditions
23 were less affected by the external temperature environment. Therefore, it can be concluded that the
24 dynamic heat transfer intensity of SR and air increased with the increase of HSI.

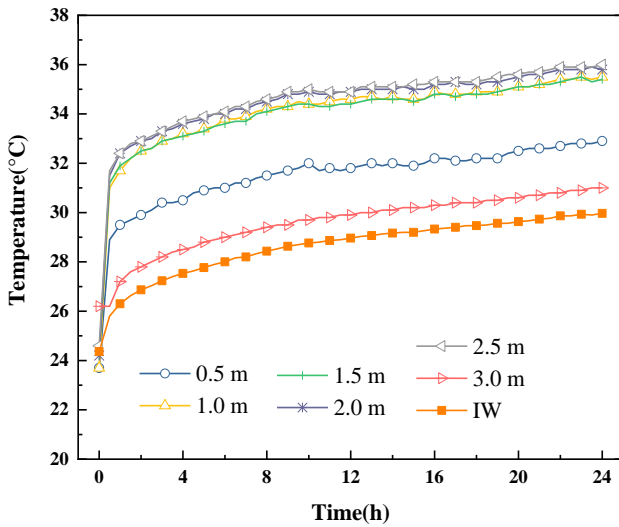
1 **3.1.2 Characteristics of IT variation under natural convection**



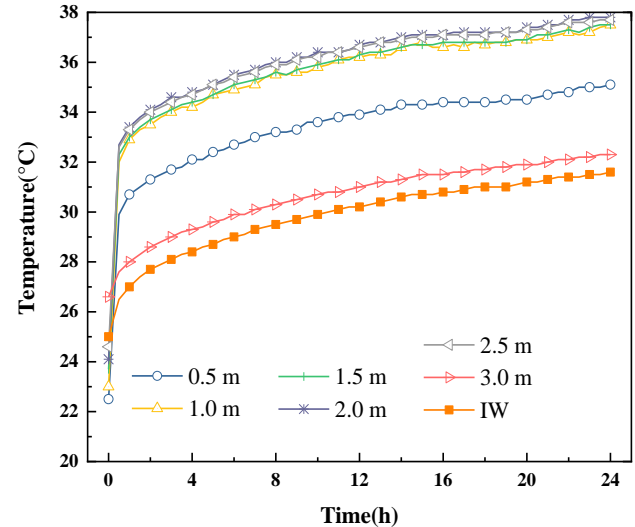
3 (a) Case1: HSI 3600 W, ISRT 21.3 °C



5 (b) Case2: HSI 4400 W, ISRT 21.7 °C



7 (c) Case3: HSI 5200 W, ISRT 21.8 °C



9 (d) Case4: HSI 6000 W, ISRT 23.1 °C

10 FIG. 7 IT changes under natural convection with different HSI

11 Fig. 7 (a) ~ (d) respectively plot the 24 h curves of IT with time for different HSI under natural
 12 convection. It can be found that under different HSI, IT increased rapidly within 0.5 h at the initial
 13 heating stage followed by a slow heating stage. In addition, it can be obviously found that the IT of the
 14 heated MRC under the condition of natural convection presented an obvious stratification phenomenon.
 From the temperature measurement points at different heights, the lowest temperature was found at
 the top 3 m. This may be due to the fact that the measurement points were closer to the top wall such
 that the measurement points were located in the laminar flow region at the wall surface. In addition,
 the average temperature of the other measuring points decreased with the increase of the height, which

1 was due to the thermal buoyancy that tended to make the hot air move upward. The air temperature at
2 the nearest 0.5 m height measurement point from the heat source was significantly lower compared
3 with other heights. For example, the temperature difference between the 0.5 m and the 2.5 m was about
4 2.5 ~ 3.0 °C. The temperature difference between the measurement points at the rest of the height was
5 within 1 °C. The phenomenon implied that reducing the position of the seat or bed as far as possible
6 can make the personnel in the MRC get better thermal comfort.

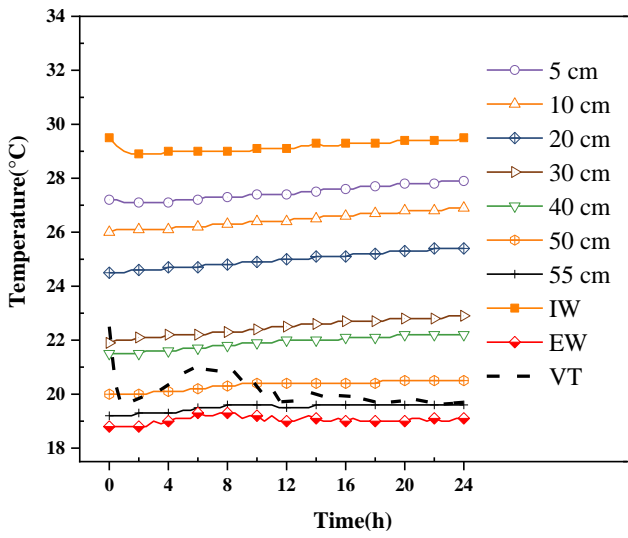
7 As can be seen from Fig. 7 (a), when the HSI is 3600 W, the maximum IT increases to 34 °C after
8 heating for 24 h. In particular, the IT at the height of 1.5 m and below where people are active during
9 the evacuation was lower than 33 °C, which satisfied the requirement that the IT should not exceed
10 35 °C. It can be predicted that the average IT may slightly exceed the allowable value range after 96 h,
11 but the temperature below 1 m level can still be controlled within 35 °C. Which indicated that for the
12 MRC with the same size as the laboratory in the current work (that is, the living room is 4 m wide and
13 12.6 m long), when there are less than 30 people in the refuge and the ISRT was lower than 21.3 °C,
14 cooling measures cannot be taken to ensure the thermal safety within 96 h.

15 Comparing Fig. 7 (b) and (c), it can be found that when the ISRT is the same, the IT increases
16 with the increase of HSI. With a HSI of 4400 W and an IRST of 21.7 ~ 21.8 °C, the IT reached a
17 maximum of 35.5 °C at 24 h and a maximum of 34.8 °C at the 1.5 m level. But when the HSI was
18 increased to 5200 W, the corresponding temperature values were 36 °C and 35.4 °C, respectively. It
19 can be seen that when the ISRT exceeded 21.7 °C and the number of people exceeded 36, natural
20 convection measures cannot not meet the requirements of temperature control in the MRC.

21 From the comparison of (a) to (d) in Fig. 7, it can be found that when the HSI increases, the
22 heating trend of the indoor and SR wall also increases significantly. When the HSI was 3600, 4400,
23 5200 and 6000 W, respectively, the average temperature at 1.5 m level at the time of 24 h increased by
24 11.9, 13.1, 13.6 and 14.3 °C, respectively, compared with the ISRT. However, the temperature
25 difference at 1 m, 1.5 m, 2 m and 2.5 m level points decreased with the increase of the HSI, which may
26 be due to the increase of the HSI made the speed of hot air uplift increase, and with the accumulation
27 of the upper airflow, the temperature grading at different heights became more blurred.

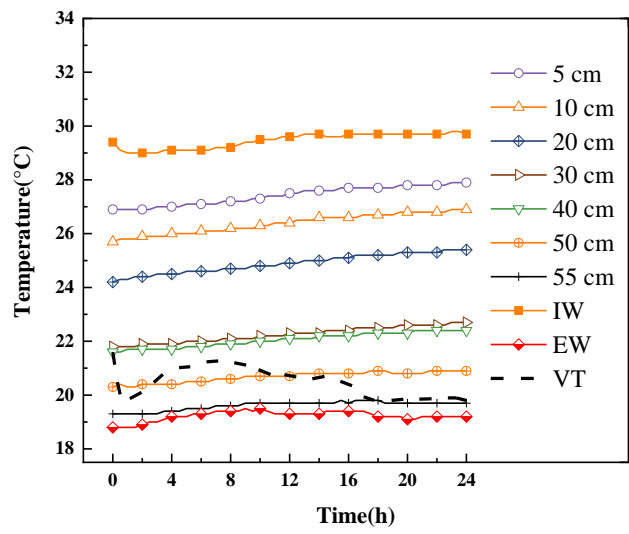
1 3.2 Temperature control characteristics of MRC under ventilation

2 3.2.1 Characteristics of SRT variation under ventilation

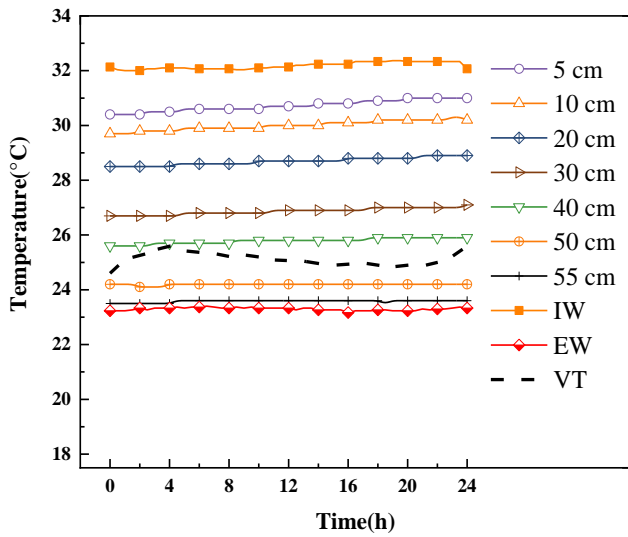


3

4 (a) Case 5: AIL II, HSI 3600 W, ISRT 23.3 °C

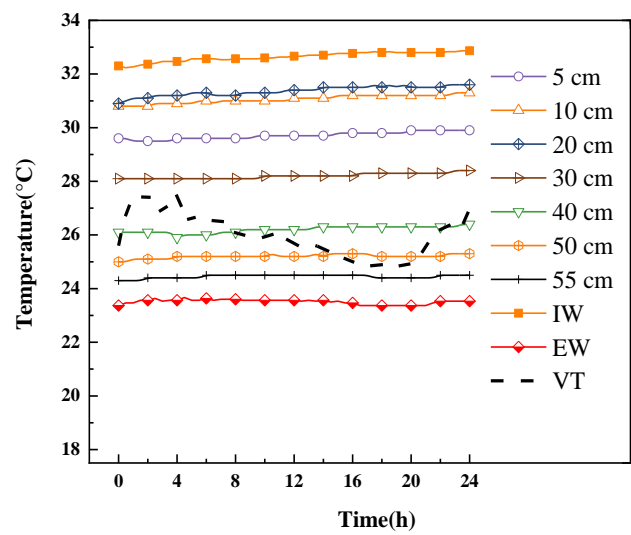


(b) Case 6: AIL III, HSI 3600 W, ISRT 23.2 °C

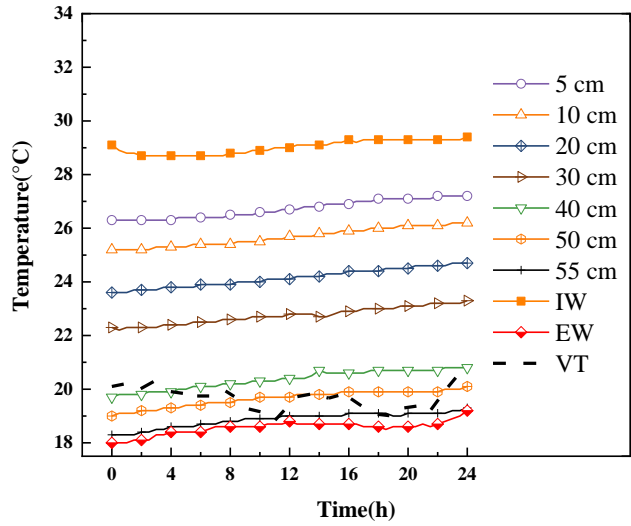
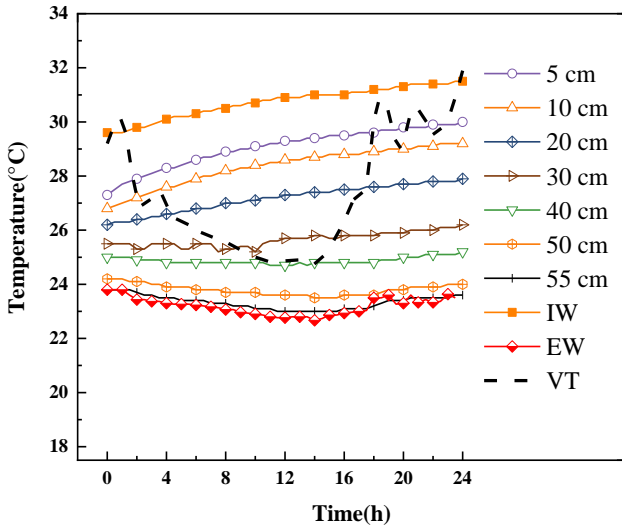


5

6 (c) Case 7: AIL I, HSI 3600 W, ISRT 27.2 °C



(d) Case 8: AIL III, HSI 3600 W, ISRT 27.6 °C

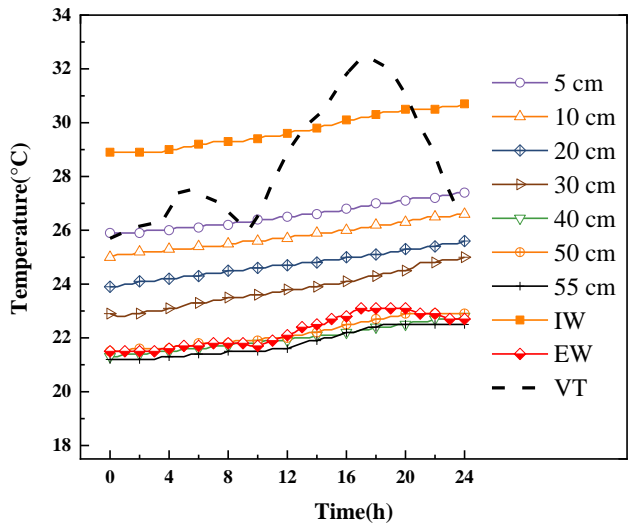
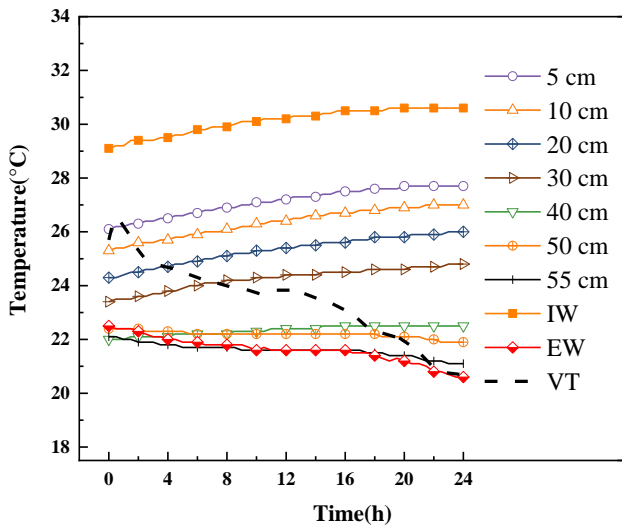


1

2

(e) Case 9: AIL I, HSI 3600 W, ISRT 25.8 °C

(f) Case 10: AIL I, HSI 4400 W, ISRT 22.5 °C



3

4

(g) Case 11: AIL I, HSI 5200 W, ISRT 23.9 °C

(h) Case 12: AIL I, HSI 6000 W, ISRT 23.3 °C

5

Fig. 8 VT and SRT change curves with time in different cases under ventilation.

6

7

8

9

10

11

12

13

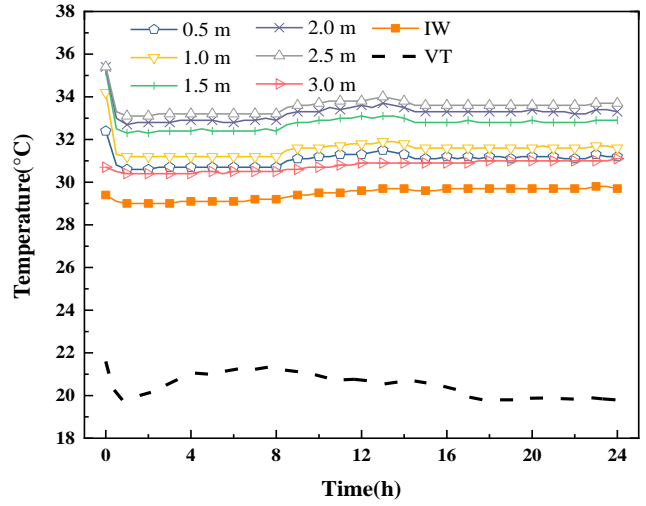
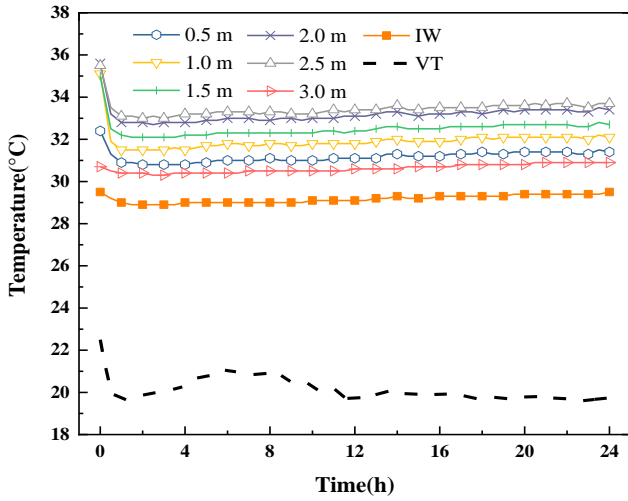
14

Fig. 8 (a) ~ (h) respectively plot the 24 h curves of SRT with time for 8 different cases under ventilation. It should be noted that the VT varies with the external environment temperature during the test process. From the VT curve in Fig. 8 (a) ~ (h), it can be seen that the VT in Cases 5, 6, 7, 8 and 10 fluctuates little with time and the temperature difference is within 3 °C, whereas the VT in Cases 9 and 12 fluctuates greatly, and the VT in Case 11 decreases approximately linearly with time over a long period of time. In addition, the ISRT of different cases was inconsistent at different depths, showing a gradual decrease in temperature from the IW to the EW face, due to the short-term heating experienced within the MRC prior to the ventilation test. In order to facilitate the analysis, the average value of different measuring points of SR at the initial time was taken as the average ISRT. The average ISRT

1 corresponding to the 8 cases was 23.3, 23.2, 27.2, 27.6, 25.8, 22.5, 23.9 and 23.3 °C, respectively. The
2 corresponding heat transfer coefficients of the 8 cases were 2.678, 2.499, 2.050, 2.612, 2.825, 2.533,
3 3.343 and 3.696 W/(m²·°C) respectively.

4 As can be seen from Fig. 8 (a) ~ (h), the SRT increases during the eight different cases, indicating
5 that the SR gained heat during the heat exchange process with the air, i.e., it has a positive effect on
6 the cooling of the MRC. It can be seen from Fig. 8 (a), (b), (c) and (d) that, when the VT is relatively
7 stable, the temperature at the measuring points 50 cm and 55 cm inside the wall hardly changes,
8 indicating that the heat influence range of SR caused by the heat exchange between indoor air and SR
9 under the ventilation is about 0.55 m. With the increase of the ISRT, the temperature gradient of IW
10 surface decreased obviously, which may be due to the decrease of the temperature difference between
11 the SR surface and the air when the ISRT increased, resulting in the weakening of the convective heat
12 exchange intensity. It can be seen from Fig. 8 (g) that the increase of the IW temperature tends to slow
13 down with the linear decrease of the VT, which is due to the reduction of the temperature difference
14 between the air and the SR after ventilation which weakens the convective heat transfer intensity. From
15 the temperature change curves in Fig. 8 (e) and (h), it can be seen that there is a large oscillation of the
16 VT during the test, but the trend of the temperature of the IW surface and the SR only changed slightly.
17 This was because the change of the VT caused a small change in IT, leading to the dynamic heat
18 transfer between the SR and air tends to balance. This phenomenon indicated that the SR played a
19 crucial role in IT control characteristics in the MRC with ventilation measures. The EW surface
20 temperature also varied slightly with the VT, which was determined by the ambient temperature of the
21 tunnel outside the refuge. In other words, the tunnel ambient temperature also affected the EW surface
22 temperature, which affected the wall temperature up to 40 cm away.

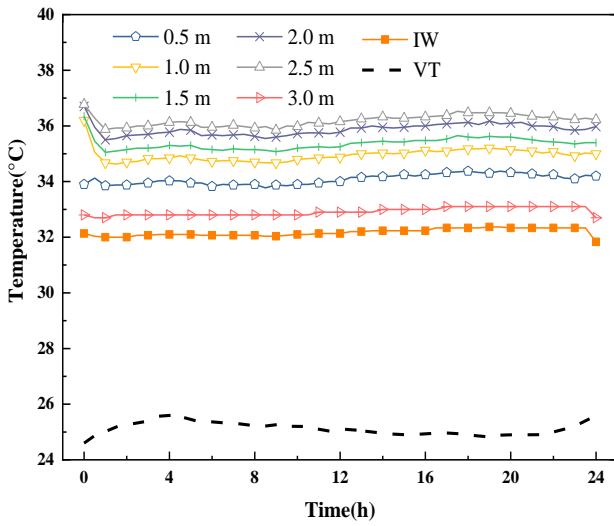
1 **3.2.2 Characteristics of IT variation under ventilation**



2

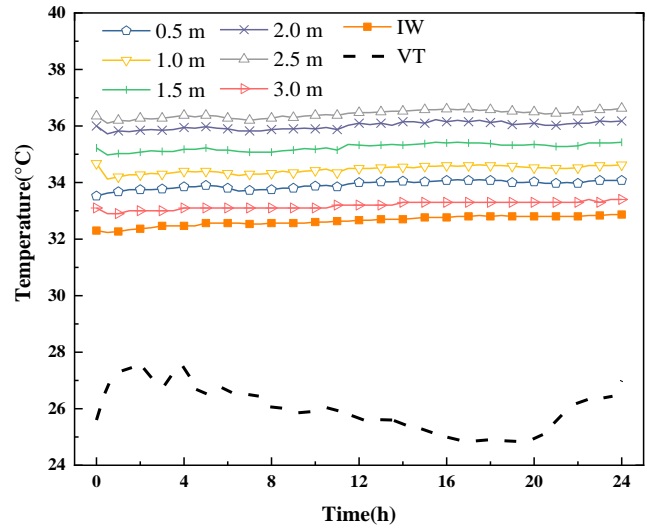
3 (a) Case5: AIL II, HSI 3600 W, ISRT 23.3 °C

(b) Case6: AIL III, HSI 3600 W, ISRT 23.2 °C

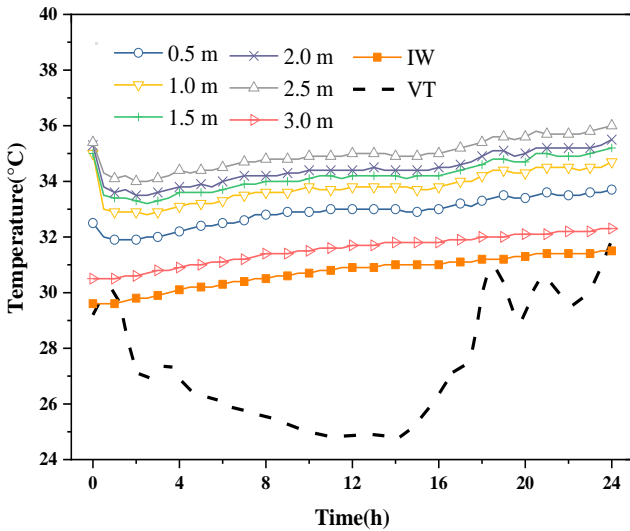


4

5 (c) Case7: AIL I, HSI 3600 W, ISRT 27.2 °C

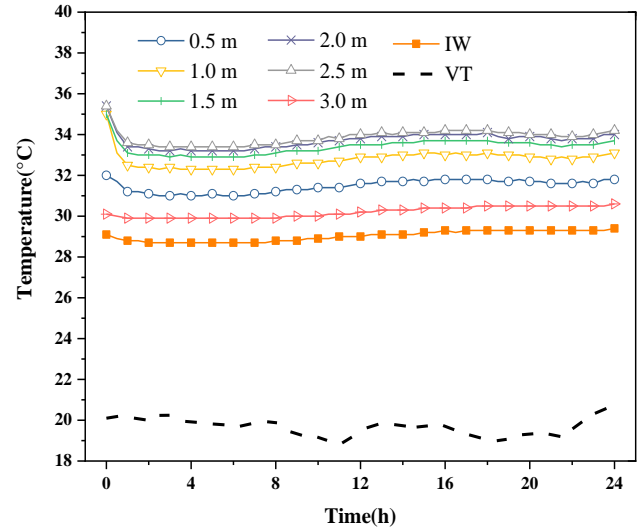


(d) Case8: AIL III, HSI 3600 W, ISRT 27.6 °C

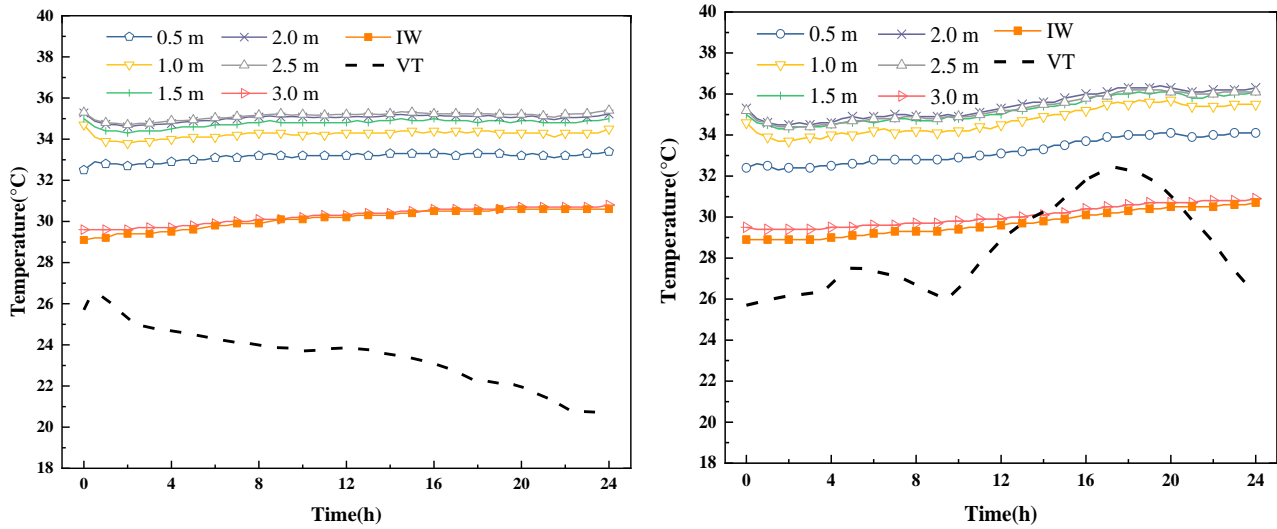


6

7 (e) Case9: AIL I, HSI 3600 W, ISRT 25.8 °C



(f) Case10: AIL I, HSI 4400 W, ISRT 22.5 °C



(g) Case11: AIL I, HSI 5200 W, ISRT 23.9 °C (h) Case12: AIL I, HSI 6000 W, ISRT 23.3 °C

Fig. 9 Variation curves of VT and IT with time in different cases under ventilation.

Fig. 9 (a) ~ (h) respectively plot the 24 h curves of VT and IT with time for 8 different cases under ventilation. It can be found that in the heated MRC with high initial IT, the IT also rapidly dropped to a relatively stable state after ventilation for about 0.5~0.8 h, indicating that the coupled heat transfer process between the SR and air also reached a dynamic equilibrium within about 0.5~0.8 h under ventilation. Secondly, it can be found that the IT was stratified with higher temperature above and lower temperature below. Compared with the temperature difference of 2.5 ~ 3 °C under natural convection, the temperature difference of 2 ~ 2.5 °C under ventilation had a more uniform IT distribution, which indicated that the ventilation can promote the uniformity of IT distribution. In addition, it can be found that the IT increases slowly when the VT is relatively stable, as shown in Fig. 9 (a), (b), (c) and (f). However, as shown in Fig. 9 (e) and (h), the influence of the VT change on the IT growth trend is relatively weak. In the case of VT change of about 5 °C, the IT change was only about 0.5 ~ 1 °C, this could be due to the transient convective heat exchange between the SR and air played a dominant role in the control of IT at the air volume of 350 m³/h. According to Fig. 9 (d) and (g), it can be found that the IT almost remains unchanged when the VT dropped approximately linearly. This indicated that under the condition of limited cooling storage capacity, reasonable operation of the risk control temperature system can make the refuge environment maintain good thermal comfort within 96 h to avoid the phenomenon of a lower IT followed by a higher one.

Comparing Fig. 9 (a) and (b), we can see that the IT trend and range of the MRC with HSI of 3600 W, ISRT of 23.2 ~ 23.3 °C, air volume of 350 m³/h and VT of about 20 °C are basically the same

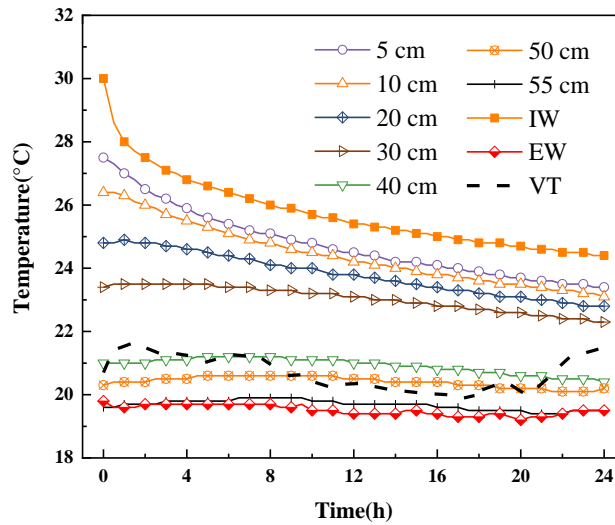
1 for the two different AILs. This meant that the IT could be kept within the range of 30.5 ~ 34 °C for
2 24 h, with only a 0.6 °C increase from 1 h to 24 h. Although AIL II obtained a more uniform IT
3 distribution than that of ventilation layout III, this difference can almost be negligible considering that
4 the temperature difference does not exceed 1 °C. By comparing Fig. 9 (c) and (d), it can be found that
5 the IT of the MRC with the HSI of 3600 W, the ISRT of 27.2 °C and 27.6 °C, the air volume of 350
6 m³/h, and the VT in the range of 25 ~ 27 °C increases by 0.5 °C from 1 h to 24 h. At the same time, the
7 maximum temperature was approximately 36 °C, and the air temperature at 1 m above ground level
8 was in the range of 34 ~ 35 °C. It showed that in the case of only 30 people in the MRC, when the
9 ISRT did not exceed 27.6 °C, the per capita air volume was 0.19 m³/min and the VT below 26 °C can
10 basically meet the temperature control requirements of the MRC. From the perspective of AIL,
11 although AIL III obtained a more uniform IT distribution than AIL I, this influence of the ventilation
12 layout also can be almost negligible considering that the temperature difference does not exceed 1 °C.

13 In addition, Fig. 9 (e) shows that a refuge with HSI of 3600 W, an ISRT of 25.8 °C, and a supply
14 air volume of 350 m³/h does not meet the 96 h temperature control requirement of 35 °C when the VT
15 exceeds 29 °C. According to Fig. 9 (f), the IT of a refuge with HSI of 4400 W, an ISRT of 22.5 °C, and
16 an air volume of 350 m³/h can be controlled to within 34 °C at a VT of approximately 20 °C. Fig. 9 (g)
17 shows that the IT can be controlled to within 35 °C for a MRC with a VT of 21 °C or less, HSI of 5200
18 W, an ISRT of 23.9 °C, and an air volume of 350 m³/h. According to Fig. 9 (h), when the air supply
19 temperature exceeds 26 °C, the IT exceeds 35 °C for a MRC with HSI of 6000 W, an ISRT of 23.3 °C
20 and an air supply volume of 350 m³/h.

21 **3.3 Cooling and heat transfer characteristics of SR under ventilation**

22 From the above analysis, it can be seen that the ISRT played a dominant role in the temperature
23 control characteristics of the MRC under the two states of natural convection and ventilation. During
24 the non-refuge period, reducing the SRT could greatly reduce the cooling load within 96 h during the
25 refuge period. In fact, the method of reducing the cooling load of the MRC by using SR storage before
26 refuge had been mentioned in Ref. [39], but the experimental research on the ventilation and cooling
27 characteristics of SR in the MRC had not been carried out due to the limitations of the test conditions.
28 This section will show the heat transfer performance of the cooling storage by SR via low-temperature
29 ventilation in the MRC, according to the test results of the Case 13.

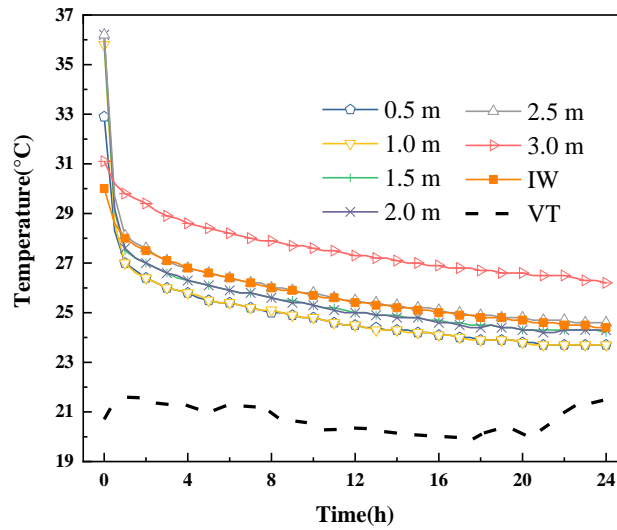
1 3.3.1 Characteristics of SRT variation during cooling storage period



2
3 Fig. 10 Variation curve of VT and SRT with time during the storage of cooling in the SR.

4 Fig. 10 plots the variation curves of the SR and VT with time when there is no heat source in the
5 MRC. From Fig. 10, the VT is relatively stable during the test period, with an average temperature of
6 20 °C and fluctuations in the range of 20 ~ 21.5 °C. The SRT decreased monotonically with time during
7 the period of ventilation and storage of the SR. The temperature of the SR inner surface in the initial
8 0.5 h of ventilation was almost linearly decreasing, and the decrease value was about 1.5 °C. After the
9 dynamic heat transfer process between the SR and air was relatively stable, the decreasing trend of the
10 IW surface temperature gradually became slower, which led to the decrease of the IW surface
11 temperature by about 4.5 °C in 1 ~ 24 h. Secondly, it can be found that the gradient of the SRT falling
12 from the inner surface decreased gradually. The temperature of the measured point at 0.4 m in the wall
13 tended to decrease during 21 ~ 24 h despite the increase of the external ambient temperature. However,
14 the temperature of the measuring point at 0.5 m remained flat during the period and then rose slightly,
15 indicating that in the process of the ventilation, the extent of the cooled SR reached 0.5 m within 24 h,
16 but the temperature at 0.4 m decreased to a lesser extent. In Fig. 6 and Fig. 8, when the MRC has an
17 internal heat source, the SR that affects the IT during natural convection and ventilation cooling is also
18 mainly located in the 0 ~ 0.4 m range. This meant that if SR storage measures are needed to reduce the
19 cooling load during the working period of the MRC, the cold source should be stored in the SR that
20 may be affected by heat transfer within 96 h during the refuge period, and the cooling amount should
21 be stored in the shallower SR as far as possible, so that the stored cold amount can be fully applied.

1 3.3.2 Characteristics of IT variation during the cooling storage period



2
3 Fig. 11. Variation curve of VT and IT with time during the storage of cooling in the SR.

4 Fig. 11 illustrates the variation curve of VT and IT with time when there is no heat source in the
5 MRC. It can be found that during the period of SR cooling, when the VT fluctuated in the range of 20
6 ~ 21.5 °C, the IT decreased monotonically with time, while the IT still showed a rapid decrease in the
7 initial 0.5 h of ventilation. When the equilibrium state of dynamic heat transfer between the SR and air
8 was reached, the decreasing gradient of IT gradually dropped, and it was basically consistent with the
9 changing trend of IW temperature. The temperature difference between the indoor and the IW surface
10 of SR is relatively close, and the temperature difference is within 1 °C. In addition, it can be found that
11 during the continuous ventilation and cooling storage period of the SR, the IT was always higher than
12 the VT, which was due to the fact that during the convective heat exchange process between the SR
13 and the air, the indoor air absorbed the heat released from the high temperature SR. Compared with
14 Figs. 7 and 9, it can be seen that the IT distribution was more uniform during the ventilation and cooling
15 storage. Except for the measuring point located at 3 m within the top laminar flow zone, the IT
16 difference of the other levels is within 1 °C, which further confirms that the upward movement of hot
17 air driven by thermal buoyancy was the main reason for IT stratification.

18 4. Discussion

19 The HSI, ventilation (determined by air supply and temperature), and SR all affect the
20 underground confined indoor thermal environment. The above experiments show that there is coupling
21 between factors, for example, the dynamic heat transfer intensity between the SR and air increases
22 with the increase of the HSI. In Case 4, that is, the temperature control experiment of MRC under

1 natural convection condition, the variation trend of IT is as expected before the experiment that the IT
2 is positively correlated with the internal heat source. Among them, the trend of Case 4 is consistent
3 with the previous experimental results of Zhang et al. [29]. Since the VT of the current experiment
4 cannot be fixed, and the VT is greater than 20 °C. This causes the IT in some Cases 5-12 to exceed the
5 required value by 35 °C. In particular, we set up different AILs in the hope of finding an optimisation
6 of the ventilation mode. However, perhaps because the space is small, the optimisation of the
7 ventilation mode is not obvious. However, in the condition of stable VT, such as Case 10, the variation
8 of IT is consistent with the simulation research trend of Zhang et al. [28]. Under Case 4, that is, the
9 experiment of the ventilation and cold storage of the SR, the temperature variation trend of the IW is
10 consistent with the experimental results of Zhang et al. [41]. The influence of the rock and soil around
11 the MRC on the temperature control can be taken into account through the IT change diagram of Case
12 4.

13 The current experiment may exist the following limitations: (1) the VT of this experiment could
14 not be fixed, and the VT was all higher than 20 °C. Therefore, the IT in some cases exceeds the required
15 value by 35 °C; (2) temperature and humidity are the main factors affecting the thermal comfort of
16 people in confined spaces, but this study did not consider the control of humidity [46]; (3) since the
17 pressure wind is applicable to shallow layers [30]. Therefore, in the face of the depletion of shallow
18 resources, in the deep temperature control, it is necessary to add daily ice storage equipment or phase
19 change refrigeration materials and other joint temperature control [47-48]; (4) due to the economy and
20 safety of spontaneous and passive temperature control of the pre-stored SR, it needs to be considered
21 to include the green cold storage carrier SR into the temperature control system. However, compared
22 with ventilation, the influence of the SR on the indoor thermal environment is slower. As shown in
23 3.1.1, after heating the MRC for 22 h, the radius of the heat regulating ring of the SR is 0.55 m. It can
24 be inferred that the cold source can be stored in the 2.4 m SR which may be affected by the heat transfer
25 within 96 h during the refuge period when the cold capacity is stored in the non-refuge period. However,
26 it is worth noting that due to the thermal deformation of the SR, the cooling amount and time required
27 for the cold storage of the SR are much greater than the cooling amount and time provided to the indoor
28 air during the refuge period. Future work will focus on exploring the heat and humidity control of the
29 underground confined space after adding the cold storage device.

1 **5. Conclusions**

2 In this study, a fully operational underground MRC capable of accommodating 30 to 50 people
3 was constructed within an underground simulated mine at a depth exceeding 2 meters. A
4 comprehensive series of experiments were conducted to investigate the temperature control
5 performance of the MRC under conditions involving natural convection and ventilation. The key
6 research findings are as follows:

7 (1) The IT gradually rises from bottom to up, and it can be more evenly distributed through
8 effective ventilation. In the case of a certain amount of ventilation, increasing the number of
9 air inlets has a weak effect on the overall trend of IT change. The heat transfer intensity
10 between SR and air increases with the increase of HSI rate and VT, while it decreases as the
11 ISRT increases.

12 (2) When considering the common temperature control of the pre-cooled SR, the cold amount
13 should be stored in the shallower SR body as far as possible to make full use of it during the
14 non-refuge period. During the evacuation period, it is recommended to reduce the VT linearly
15 to ensure the thermal safety of personnel.

16 (3) In the case of a test MRC with a capacity below 30 people and an IRST below 21.3 °C, it is
17 not possible to implement the cooling measures to ensure thermal safety for a duration of 96
18 h. In addition, if the IRST is lower than 27.6 °C, employing pressure air supply with per capita
19 air volume exceeding 0.19 m³/min and VT below 26 °C can effectively meet the demand.

20 (4) When the capacity falls below 43 people and the IRST remains under 23.9 °C, maintaining
21 per capita air volume above 0.14 m³/min along with VT lower than or equal to 21 °C would
22 be sufficient for ensuring thermal comfort during 96 h.

23 **Credit authorship contribution statement**

24 **Zujing Zhang:** Supervision, Funding acquisition, Formal analysis, Project administration,
25 Conceptualization, Writing – review & editing. **Ting Jin:** Conceptualization, Writing – original draft,
26 Data curation, Investigation. **Liang Ge:** Resources, Methodology. **Xing Liang:** Formal analysis,
27 Methodology. **Hongwei Wu:** Formal analysis, Writing – review & editing. **Ruiyong Mao:** Formal
28 analysis, Investigation.
29

1 **Acknowledgments**

2 The authors would like to thank the financial support from the National Natural Science
3 Foundation of China (52168013), the Guizhou Provincial Science and Technology Projects
4 (ZK[2022]151) and the State Key Laboratory of Gas Disaster Detecting, Preventing and Emergency
5 Controlling Open-fund Project (2021SKLKF10).

6 **References:**

- 7 [1] L.J. Sun, J.W. Leng, Research on influencing factors of travel in underground space based on multi-
8 source data: Spatial optimization design for low-carbon travel, *Energ Buildings* 253 (2021).
9 <https://doi.org/10.1016/j.enbuild.2021.111524>.
- 10 [2] Y.Y. Wu, X.D. Chen, H. Li, X. Zhang, X. Yan, X. Dong, X.T. Li, B. Cao, Influence of thermal
11 and lighting factors on human perception and work performance in simulated underground
12 environment, *Sci Total Environ* 828 (2022). <https://doi.org/10.1016/j.scitotenv.2022.154455>.
- 13 [3] J. Li, W. Wu, Y. Jin, R. Zhao, W. Bian, Research on environmental comfort and cognitive
14 performance based on EEG+VR+LEC evaluation method in underground space, *Build Environ*
15 198 (2021) 107886. <https://doi.org/10.1016/j.buildenv.2021.107886>.
- 16 [4] B. Hebbal, Y. Marif, M. Hamdani, M.M. Belhadj, H. Bouguettaia, D. Bechki, The geothermal
17 potential of underground buildings in hot climates: Case of Southern Algeria, *Case Stud Therm*
18 *Eng* 28 (2021) 101422. <https://doi.org/10.1016/j.csite.2021.101422>.
- 19 [5] L. Chen, Q. Shi, Experimental study and performance analysis on a closed-cycle rotary
20 dehumidification air conditioning system in deep underground spaces, *Case Stud Therm Eng* 37
21 (2022) 102245. <https://doi.org/10.1016/j.csite.2022.102245>.
- 22 [6] C. Ma, F. Peng, Y. Qiao, H. Li, Influential factors of spatial performance in metro-led urban
23 underground public space: A case study in Shanghai, *Undergr Space* 8 (2023) 229-251.
24 <https://doi.org/10.1016/j.undsp.2022.03.001>.
- 25 [7] M. Bettelini, Systems approach to underground safety, *Undergr Space* 5(3) (2020) 258-266.
26 <https://doi.org/10.1016/j.undsp.2019.04.005>.
- 27 [8] W.Z. Lu, Y.Z. Wu, C.L. Choguill, S.K. Lai, J.J. Luo, Underground Hangzhou: The challenge of
28 safety vs. commerciality in a major Chinese city, *Cities* 119 (2021).
29 <https://doi.org/10.1016/j.cities.2021.103414>.

- 1 [9] L.L. Dong, Y.F. He, Q.L. Qi, W. Wang, Optimization of daylight in atrium in underground
2 commercial spaces: A case study in Chongqing, China, *Energ Buildings* 256 (2022).
3 <https://doi.org/10.1016/j.enbuild.2021.111739>.
- 4 [10] W. Broere, Urban underground space: Solving the problems of today's cities, *Tunn Undergr Sp*
5 *Tech* 55 (2016) 245-248. <https://doi.org/10.1016/j.tust.2015.11.012>.
- 6 [11] Y. Li, S.B. Geng, X.S. Zhang, H. Zhang, Study of thermal comfort in underground construction
7 based on field measurements and questionnaires in China, *Build Environ* 116 (2017) 45-54.
8 <https://doi.org/10.1016/j.buildenv.2017.02.003>.
- 9 [12] J.T. Lin, Y.H. Kong, L. Zhong, Optimization of environment control system for narrow sleeping
10 space in underground shelters, *Energ Buildings* 263 (2022).
11 <https://doi.org/10.1016/j.enbuild.2022.112043>.
- 12 [13] J.G. Jin, Y.F. Shen, H. Hu, Y.Q. Fan, M.J. Yu, Optimizing underground shelter location and mass
13 pedestrian evacuation in urban community areas: A case study of Shanghai, *Transport Res a-Pol*
14 149 (2021) 124-138. <https://doi.org/10.1016/j.tra.2021.04.009>.
- 15 [14] K.E. Karadeniz, S. Nowak, D. Guner, T. Sherizadeh, Evaluation on Underground Refuge
16 Alternatives and Explosion Survivability: a Review, *Mining Metall Explor* 39(6) (2022) 2311-
17 2331. <https://doi.org/10.1007/s42461-022-00682-1>.
- 18 [15] Y. Wang, Y.Y. Wang, S.M. Li, N. Qin, P. Du, T.T. Zhou, Research on the Novel Honeycomb-
19 Like Cabin Based on Computer Simulation, *Comput Syst Sci Eng* 39(2) (2021) 179-195.
20 <https://doi.org/10.32604/csse.2021.014469>.
- 21 [16] S. Wang, L.Z. Jin, S.N. Ou, Y.G. Li, Experimental air curtain solution for refuge alternatives in
22 underground mines, *Tunn Undergr Sp Tech* 68 (2017) 74-81.
23 <https://doi.org/10.1016/j.tust.2017.05.024>.
- 24 [17] C. Zeng, Y.P. Yuan, B. Xiang, X.L. Cao, Z.L. Zhang, L.L. Sun, Thermal and infrared camouflage
25 performance of earth-air heat exchanger for cooling an underground diesel generator room for
26 protective engineering, *Sustain Cities Soc* 47 (2019). <https://doi.org/10.1016/j.scs.2019.101437>.
- 27 [18] J. Yu, Y.M. Kang, Z.Q. Zhai, Advances in research for underground buildings: Energy, thermal
28 comfort and indoor air quality, *Energ Buildings* 215 (2020).
29 <https://doi.org/10.1016/j.enbuild.2020.109916>.

- 1 [19] D.S. Yantek, L. Yan, P.T. Bissert, M.D. Klein, Effects of mine strata thermal behavior and mine
2 initial temperatures on mobile refuge alternative temperature., *Mining engineering* 69(4) (2017)
3 41-48. <https://doi.org/10.19150/me.7393>.
- 4 [20] L.C. Yan, D. Yantek, T. Lutz, J. Yonkey, J. Srednicki, Underground Mine Refuge Alternatives
5 Heat Mitigation, *J Therm Sci Eng Appl* 12(2) (2020). <https://doi.org/10.1115/1.4044345>.
- 6 [21] Y. Li, S. Li, W. Gao, W. Xu, Y. Xu, J. Wang, Exploring the effects of IT on college students'
7 physiological responses, cognitive performance and a concentration index derived from EEG
8 signals, *Dev Built Environ* 12 (2022) 100095. <https://doi.org/10.1016/j.dibe.2022.100095>.
- 9 [22] Z. Zhang, W. Guo, R. Mao, L. Ge, X. Liang, H. Wu, Performance analysis of an improved
10 temperature control scheme with cold stored in surrounding rock for underground refuge chamber,
11 *Appl Therm Eng* (2023) 121589. <https://doi.org/10.1016/j.applthermaleng.2023.121589>.
- 12 [23] Z. Zhang, W. Guo, X. Gao, H. Wu, R. Mao, Investigation on temperature control based on cooled
13 mine compressed air for mine refuge chamber with high-temperature surrounding rock, *Int J*
14 *Therm Sci* 187 (2023) 108201. <https://doi.org/10.1016/j.ijthermalsci.2023.108201>.
- 15 [24] D.S. Yantek, H.E. Camargo, P. Jurovcik, Noise and vibration assessment of a roof bolting
16 machine, *Noise Control Eng J* 58(6) (2010) 601-610. <https://doi.org/10.3397/1.3495738>.
- 17 [25] T.E. Bernard, D.S. Yantek, E.D. Thimons, Estimation of metabolic heat input for refuge
18 alternative thermal testing and simulation., *Mining engineering* 70(8) (2018) 50-54.
19 <https://doi.org/10.19150/me.8429>.
- 20 [26] B. Wu, B. Lei, C. Zhou, Z. Zhao, Experimental Study of Phase Change Material's Application in
21 Refuge Chamber of Coal Mine, *Procedia Engineering* 45 (2012) 936-941.
22 <https://doi.org/10.1016/j.proeng.2012.08.262>.
- 23 [27] Z.J. Zhang, T. Jin, H.W. Wu, R. Day, X.K. Gao, K.Q. Wang, R.Y. Mao, Experimental
24 investigation on environmental control of a 50-person mine refuge chamber, *Build Environ* 210
25 (2022). <https://doi.org/10.1016/j.buildenv.2021.108667>.
- 26 [28] Z.J. Zhang, H.W. Wu, K.Q. Wang, R. Day, Y.P. Yuan, Thermal performance of a mine refuge
27 chamber with human body heat sources under ventilation, *Appl Therm Eng* 162 (2019).
28 <https://doi.org/10.1016/j.applthermaleng.2019.114243>.

- 1 [29] Z.J. Zhang, R. Day, K.Q. Wang, H.W. Wu, Y.P. Yuan, Thermal performance analysis of an
2 underground closed chamber with human body heat sources under natural convection, *Appl*
3 *Therm Eng* 145 (2018) 453-463. <https://doi.org/10.1016/j.applthermaleng.2018.09.068>.
- 4 [30] X.K. Gao, Z.J. Zhang, Y.M. Xiao, Modelling and thermo-hygrometric performance study of an
5 underground chamber with a long vertical earth-air heat exchanger system, *Appl Therm Eng* 180
6 (2020). <https://doi.org/10.1016/j.applthermaleng.2020.115773>.
- 7 [31] A.A. Abdelfattah, E.Z. Ibrahim, S.A.E. Sayed Ahmed, W.M. Elwan, M.L. Elsayed, M.A.
8 Abdelatif, Thermal performance augmentation of a semi-circular cylinder in crossflow using
9 longitudinal fins, *Int Commun Heat Mass* 125 (2021) 105159.
10 <https://doi.org/10.1016/j.icheatmasstransfer.2021.105159>.
- 11 [32] A. Afifi, H. Zawati, E.Z. Ibrahim, M.L. Elsayed, M.A. Abdelatif, Assessment strategy for a
12 longitudinally finned semi-circular tube bank, *Int Commun Heat Mass* 139 (2022) 106489.
13 <https://doi.org/10.1016/j.icheatmasstransfer.2022.106489>.
- 14 [33] I.A. Mahmoud, M.A. Saleh, O.M. Mesalhy, E.F. Mohamed, M.A. Abdelatif, Hollow trapezoidal
15 baffles in a rectangular channel: Thermal/hydraulic assessment with ANN numerical approach,
16 *Int Commun Heat Mass* 139 (2022) 106505.
17 <https://doi.org/10.1016/j.icheatmasstransfer.2022.106505>.
- 18 [34] K. Wang, Q. Li, J. Wang, S. Yang, Thermodynamic characteristics of deep space: hot hazard
19 control case study in 1010-m-deep mine, *Case Stud Therm Eng* 28 (2021) 101656.
20 <https://doi.org/10.1016/j.csite.2021.101656>.
- 21 [35] J. Li, L. Wu, H. Chen, Analysis of thermal comfort and threshold range of airflow supply
22 parameters for different types of work in humid-heat coal mines, *Case Stud Therm Eng* 44 (2023)
23 102826. <https://doi.org/10.1016/j.csite.2023.102826>.
- 24 [36] F. Marongiu, S. Soprani, K. Engelbrecht, Modeling of high temperature thermal energy storage
25 in rock beds - Experimental comparison and parametric study, *Appl Therm Eng* 163 (2019).
26 <https://doi.org/10.1016/j.applthermaleng.2019.114355>.
- 27 [37] S.A. Ghoreishi-Madiseh, A.P. Sasmito, F.P. Hassani, L. Amiri, Performance evaluation of large
28 scale rock-pit seasonal thermal energy storage for application in underground mine ventilation,
29 *Appl Energy* 185 (2017) 1940-1947. <https://doi.org/10.1016/j.apenergy.2016.01.062>.

- 1 [38] S. Zhu, J.W. Cheng, W.T. Song, M. Borowski, Y.J. Zhang, B.H. Yu, Y. Wang, C. Qi, P. Tukkaraja,
2 G. Hua, Y.G. Xu, A. Ghosh, C. Wang, Y. Peng, Using seasonal temperature difference in
3 underground surrounding rocks to cooling ventilation airflow: A conceptual model and simulation
4 study, *Energy Sci Eng* 8(10) (2020) 3457-3475. <https://doi.org/10.1002/ese3.619>.
- 5 [39] Y. Yuan, X. Gao, H. Wu, Z. Zhang, X. Cao, L. Sun, N. Yu, Coupled cooling method and
6 application of latent heat thermal energy storage combined with pre-cooling of envelope: Method
7 and model development, *Energy* 119 (2017) 817-833.
8 <https://doi.org/10.1016/j.energy.2016.11.058>.
- 9 [40] X.K. Gao, Y.P. Yuan, H.W. Wu, X.L. Cao, X.D. Zhao, Coupled cooling method and application
10 of latent heat thermal energy storage combined with pre-cooling of envelope: Optimization of
11 pre-cooling with intermittent mode, *Sustain Cities Soc* 38 (2018) 370-381.
12 <https://doi.org/10.1016/j.scs.2018.01.014>.
- 13 [41] Y. Zhang, Z.J. Wan, B. Gu, C.B. Zhou, An experimental investigation of transient heat transfer
14 in surrounding rock mass of high geothermal roadway, *Therm Sci* 20(6) (2016) 2149-2158.
15 <https://doi.org/10.2298/TSCI151017053Z>.
- 16 [42] W. Dingyi, D. Cuifeng, X. Haiyue, Z. Lianfu, Influencing factors and correlation analysis of
17 ventilation and cooling in deep excavation roadway, *Case Stud Therm Eng* 14 (2019) 100483.
18 <https://doi.org/10.1016/j.csite.2019.100483>.
- 19 [43] Z.J. Zhang, H.W. Wu, K.Q. Wang, R. Day, Y.P. Yuan, Air quality control in mine refuge chamber
20 with ventilation through pressure air pipeline, *Process Saf Environ* 135 (2020) 46-58.
21 <https://doi.org/10.1016/j.psep.2019.12.014>.
- 22 [44] China Academy of Building Science. Code for Thermal Design of Civil Buildings: GB 50176-
23 2016 [S]. Beijing: China Building and Construction Press, 2016.
- 24 [45] T. Taner, Energy and exergy analyze of PEM fuel cell: A case study of modeling and simulations,
25 *Energy* 143 (2018) 284-294. <https://doi.org/10.1016/j.energy.2017.10.102>.
- 26 [46] Y. Li, Y.P. Yuan, C.F. Li, X. Han, X.S. Zhang, Human responses to high air temperature, relative
27 humidity and carbon dioxide concentration in underground refuge chamber, *Build Environ* 131
28 (2018) 53-62. <https://doi.org/10.1016/j.buildenv.2017.12.038>.

- 1 [47] S. Wang, W. Wang, K. Shao, W. Ding, Z. Cui, W. Shao, W. Ji, Operation optimization of a
2 refrigeration ventilation system for the deep metal mine, *Case Stud Therm Eng* 44 (2023) 102817.
3 <https://doi.org/10.1016/j.csite.2023.102817>.
- 4 [48] X.K. Gao, Y.P. Yuan, X.L. Cao, H.W. Wu, X.D. Zhao, D. Yan, Coupled cooling method and
5 application of latent heat thermal energy storage combined with pre-cooling of envelope:
6 Temperature control using phase-change chair, *Sustain Cities Soc* 42 (2018) 38-51.
7 <https://doi.org/10.1016/j.scs.2018.06.032>.

8